

CYCLIC POLARIZATION RESISTANCE MEASUREMENTS OF CONCRETE REINFORCING STEEL WITH CONSTANT PHASE ANGLE ELEMENT CHARGE STORAGE BEHAVIOR

A. A. Sagüés, S. C. Kranc and E. I. Moreno*
Department of Civil and Environmental Engineering
University of South Florida
Tampa Florida 33620
*Permanent Affiliation: CINVESTAV-Mérida, México

ABSTRACT

Many corroding interfaces exhibit electrochemical impedance response similar to that of a polarization resistance associated with the corrosion process, in parallel with a Constant Phase Angle Element (CPE) having relatively large admittance. Such conditions are often encountered in the case of steel in concrete. While polarization measurements using a forward and reverse potential scan rate dV/dt can be helpful to subtract the contribution of an ideal interfacial capacitance C by using a $C dV/dt$ correction, in concrete the pronounced frequency dispersion of the CPE complicates the time domain response and correction is not straightforward. A solution to the problem is presented in this paper and applied to evaluate the CPE parameters and estimate the polarization resistance of steel in concrete from cyclic-scan polarization measurements. The technique is demonstrated for experiments with plain steel and galvanized rebar in concrete.

Keywords: concrete, corrosion, constant phase angle element, cyclic polarization, modeling, reinforcing steel.

INTRODUCTION

The measurement of small corrosion rates of reinforcing steel in concrete is complicated by the presence of an interfacial charge storage mechanism that resembles a large, highly non-ideal capacitance.¹⁻³ Conventional Polarization Resistance (PR) measurement methods⁴ involve imposing

Copyright

a small potentiostatic excursion at a constant potential scan rate (\dot{V}), and recording the current demand I . Correction for solution resistance (R_s) is performed automatically during the test or as a postprocessing step if an independent measurement of R_s is made. The potential excursion is usually made either in the negative direction from the open circuit potential or in the positive direction from a few mV below the open circuit potential. The apparent polarization resistance, defined as the slope of the potential-current curve ($R_{pa} = dE/dI$), is then evaluated for the end of the potential excursion or for the open circuit potential. R_{pa} is area-normalized by multiplying by the nominal steel area in contact with the concrete. For relatively high corrosion current densities ($i_{corr} \geq 1 \mu A/cm^2$) and moderate \dot{V} values (0.1 mV/s) the portion of the current demand introduced by the interfacial charge storage mechanism is normally only a small fraction of the total current at the point where the slope is evaluated. However, when i_{corr} is significantly less than $1 \mu A/cm^2$ (including the borderline range between actively corroding and passive steel conditions)⁵ the current demand of the interfacial charge storage mechanism is relatively large and the apparent polarization resistance may become strongly dependent on \dot{V} . Impractically low values of \dot{V} may be required to obtain results that approximate the actual polarization resistance of the system.

Methods for processing PR data to extract the effect of the presence of interfacial capacitance in experiments of finite duration have been developed in the past for cases when ideal capacitive behavior is present^{6,7}. However as indicated previously, the charge storage behavior is quite unlike that of an ideal capacitor and can be treated instead as that of a constant phase angle element (CPE), especially in the frequency range $1 \text{ mHz} < f < 100 \text{ mHz}$. That portion of the frequency domain, typically sampled in the time domain by the PR technique, is where much of the useful corrosion reaction rate information resides. Calculations in the time domain to compensate for current demand by a CPE have only recently been introduced, for the case of PR measurements with unidirectional potential scan¹, and for galvanostatic step polarization experiments^{2,3}.

Cyclic PR experiments (CYCPR), consisting of a forward and a reverse potential scan returning to the original condition, can be useful in revealing the presence and relative importance of interfacial charge storage in a corrosion test. Behavior under cyclic PR has been examined in the literature, but again primarily for systems with ideal capacitance^{6,7}. In this paper, calculations and experiments are presented to quantify the response of steel in concrete for single-cycle CYCPR experiments. The goal of the investigation is to provide the basis for improved evaluation of the actual polarization resistance of a system exhibiting a combination of CPE charge storage behavior, coupled with simple polarization and solution resistances.

EXPERIMENTAL METHOD

Reinforced concrete specimens from an ongoing investigation into the behavior of plain and galvanized steel in concrete,⁸ were selected for experimental testing and application of the theoretical treatment to the results. The specimens were rectangular in shape, 75 x 150 x 300 mm, with two embedded reinforcing bars (12.5 mm in diameter) placed longitudinally 75 mm apart, with an effective unmasked length of 200 mm (metal area in contact with concrete $\sim 80 \text{ cm}^2$). The selected specimens were from three concrete mix formulations made using Portland cement type II, a nominal water-to-binder ratio of 0.40, and different pozzolanic replacement as follows: mix 1 (20% fly ash), mix 2 (30% fly ash), and mix 3 (20% fly ash + 8% silica fume). A total of 5 specimens were examined, 3 with galvanized and 2 with plain steel bars. No chloride additions were made, and the specimens had been kept nearly saturated in fresh water inside plastic bags for ~ 1100 days following the end of a 28 day moist cure. For the electrochemical tests, one bar was used as the working electrode and the other bar was used as the auxiliary electrode. An activated

Ti rod (ATR) reference electrode (50 mm long) was embedded between the bars.⁹ EIS tests were conducted using an EG&G PARC Model 378⁽¹⁾ system at an amplitude typically less than 10 mV, in the frequency interval 0.001 - 1,000 Hz. CYCPR tests were conducted with a GAMRY CMS 100⁽¹⁾ system by varying the potential (starting from the open circuit value) in the negative direction, at scan rates of 0.0125 mV s⁻¹ and 0.05 mV s⁻¹. The direction was reversed when the potential reached 10 mV below the starting potential. The ohmic resistance compensation system was disabled during the tests. The apparent polarization resistance was obtained from the slope of the potential-current curve at the maximum potential deviation and upon return to the initial potential. All polarization parameters are presented without surface normalization, which can be calculated by multiplying/dividing as appropriate by the nominal specimen metal area (80 cm²). The specimens were allowed to rest between tests until the open circuit potential returned to the initial value. The concrete solution resistance in the cyclic polarization resistance tests was determined independently by single frequency A.C. measurements using a soil resistivity meter operating with a square wave at 97 Hz. The two current terminals were connected one to the working and the other to the counter electrode. The corresponding potential-sense electrodes were connected to the working and reference electrodes respectively.

RESULTS

Figures 1 and 2 show typical EIS responses (plain steel and galvanized steel respectively) of the specimens investigated. The impedance diagrams are typical of systems experiencing very low corrosion rates. This is in agreement with the exposure conditions (mature concrete, no chloride ion contamination and minimal carbonation of the concrete), and with the metal potentials which are in the expected range for passive surface conditions.¹⁰ The approximation to nearly ideal CPE behavior in parallel with a very large polarization resistance in the frequency range 1 mHz-100 mHz is evident in both diagrams, after allowing for the presence of a solution resistance R_s . Analysis of the results with the commercial program EQUIVCRT⁽¹⁾ yielded best-fit values for the CPE parameters n and Y_o (see Discussion section), the polarization resistance R_p and the solution resistance R_s . Multiple tests of the same specimens yielded consistently similar behavior. The averages of the parameters (inverse of average of R_p^{-1} in the case of the polarization resistances) obtained for each specimen are listed in Tables 1 and 2.

Figures 3 and 4 show the results of cyclic polarization experiments performed for the same specimens of Figures 1 and 2. The points corresponding to the ends of the downward and return scans are indicated. The diagrams show strong hysteresis that became more pronounced at the highest scan rate. Behavior similar to that shown in Figures 3 and 4 was observed consistently in multiple tests with these and the other specimens. The currents corresponding to the beginning of the tests were not exactly zero in all cases because of minute fluctuations in the open circuit potential measurements used to establish E_{corr} before the initiation of the test. As a result, potentiostatic control sometimes imposed a very small potential step when first established, with a consequent brief capacitive current transient.

Examination of the cyclic polarization results (after correction for the relatively small effect of ohmic solution resistance) showed apparent polarization resistance R_{pa} values (Table 2) that decreased substantially as the value of the scan rate increased by a factor of 4. This strong dependence was present regardless of whether R_{pa} was defined variously by the slope of the curve at the end of the negative-going scan, or near E_{corr} during the return scan. The dependence of R_{pa}

⁽¹⁾ Tradename

on \dot{V} is in agreement with the significantly non-ideal capacitive behavior of the interface revealed by the EIS results.

DISCUSSION

Theoretical examination of the time domain behavior.

The following derivation was conducted in an attempt to develop a simple analysis of the time domain data to provide estimates of the magnitude of the interfacial charge storage parameters and the polarization resistance, without the need for independent EIS testing.

The calculations were restricted to systems in which the metal-electrolyte interface, under small-signal excitation of frequency $f = \omega/2\pi$, behaves approximately as a polarization resistance R_p in parallel with a CPE (Figure 5). The CPE has impedance $Z_{CPE} = Y_o^{-1} (j\omega)^{-n}$,^{1-3,11,12} with a phase angle which is frequency-independent and equal to $-n\pi/2$, where $0 < n < 1$. Y_o is the magnitude of the admittance of the CPE at a frequency of $1/2\pi$ Hz. The time domain response of the CPE can be obtained by envisioning any arbitrary potential excitation as the sum of infinitesimal individual potential steps of variable amplitude and applied successively. Simple linear superposition is assumed. The response to an individual potential step can be obtained by transformation from the frequency domain impedance using standard techniques.¹³ Thus, for the CPE, the current response for a unit-amplitude potential step is

$$A(t) = Y_o t^{-n} / \Gamma(1-n) \quad (1)$$

where Γ is Euler's Gamma function, found in standard mathematical tables.

As shown in Ref.[1], the current demand response $I_{CPE}(t)$ of a CPE to a potential excitation ramp of scan rate $\pm \dot{V}$ starting from a previously steady value $V=0$ at time $t=0$ is given by

$$I_{CPE}(t) \Big|_{t>0} = \pm Y_o \dot{V} t^{1-n} / (1-n) \Gamma(1-n) \quad (2)$$

Eq. (2) can be used to advantage to examine the effect of the waveform $V(t)$ shown in Figure 6, which corresponds to the potential excitation schedule (neglecting for now solution resistance effects) used to produce the data in Figs. 3 and 4. $V(t)$ can be considered as the sum of the two ramps $V_1(t)$ and $V_2(t)$ shown by dashed lines in Fig. 6. The maximum potential excursion from E_{corr} is $V_{MAX} = -\dot{V} T/2$, where $T/2$ is the duration of the downward potential scan. Notice that for convenience V_{MAX} is defined as a negative number in this treatment tailored to cathodic scans. By invoking linear superposition and application of Eq(2) one obtains

$$I_{CPE}(t) \Big|_{t>0} = I_1(t) + I_2(t) \quad (2a)$$

$$I_1(t) \Big|_{t>0} = -Y_o \dot{V} t^{1-n} / (1-n) \Gamma(1-n) \quad (2b)$$

$$I_2(t) \Big|_{t>T/2} = 2Y_o \dot{V} (t-T/2)^{1-n} / (1-n) \Gamma(1-n) \quad (2c)$$

$$I_2(t) \Big|_{t<T/2} = 0 \quad (2d)$$

The total current demand for the interface I_T is given by the sum of the current demands of the CPE and the polarization admittance R_p^{-1}

$$I_T = I_{CPE}(t) + V(t) R_p^{-1} \quad (3)$$

At the end of the downward scan, just before the beginning of the upward scan ($t=T/2-0$), the total current I_D is

$$I_D = I_T(T/2-0) = -Y_o \dot{V} (T/2)^{1-n} / (1-n) \Gamma(1-n) + V_{MAX} R_p^{-1} \quad (4)$$

At the end of the return scan, when E_{corr} is reached again, the total current I_E is

$$\begin{aligned} I_E &= I_T(T) = Y_o \dot{V} [2(T/2)^{1-n} - T^{1-n}] / (1-n) \Gamma(1-n) \\ &= Y_o \dot{V} T^{1-n} (2^n - 1) / (1-n) \Gamma(1-n) = Y_o \dot{V} T^{1-n} f(n) \end{aligned} \quad (5)$$

$$f(n) = (2^n - 1) / (1-n) \Gamma(1-n) \quad (5a)$$

Notice that since I_E is obtained at E_{corr} , there is no contribution to I_E from the polarization admittance. Therefore, the values I_{EA} and I_{EB} measured at two different scan rates \dot{V}_A and \dot{V}_B could be used to set up a system of two equations in the form Eq.(5) and solve for n and Y_o . R_p can then be obtained by replacing those values in Eq.(4).

Since n and Y_o are assumed to be properties of the CPE and thus scan rate invariant

$$I_{EA}/I_{EB} = \dot{V}_A T_A^{1-n} / \dot{V}_B T_B^{1-n} \quad (6)$$

By taking logarithm of both sides and recalling that $V_{MAX} = -\dot{V} T/2$

$$n = \log(I_{EA} V_{MAXB} / I_{EB} V_{MAXA}) / \log(\dot{V}_A V_{MAXB} / \dot{V}_B V_{MAXA}) \quad (7)$$

Or if V_{MAX} is the same in both tests

$$n = \log(I_{EA} / I_{EB}) / \log(\dot{V}_A / \dot{V}_B) \quad (8)$$

Eq(5) can then be used to solve for Y_o by inserting the value of n together with I_{EA} , \dot{V}_A , and $T_A = -2V_{MAXA}/\dot{V}_A$ (or the corresponding magnitudes for test B).

$$Y_o = I_{EA} \dot{V}_A^{-n} (-V_{MAXA})^{n-1} 2^{n-1} (f(n))^{-1} = I_{EB} \dot{V}_B^{-n} (-V_{MAXB})^{n-1} 2^{n-1} (f(n))^{-1} \quad (9)$$

A value for R_p can then be obtained for tests A and B by using the parameters corresponding to each test, and inserting the values in the following expression obtained by rearranging Eq.(4)

$$R_p = V_{MAX} / (I_D + Y_o \dot{V} (-V_{MAX})^{1-n} f(n) (2^n - 1)^{-1}) \quad (10)$$

It should be noted that whereas n and Y_o are uniquely determined by Eqs.(7) and (9), R_p is not mathematically constrained to be the same when test A or test B are used for evaluation. Differences between the values obtained for R_p when using the results of both tests may give an indication of the sensitivity of the results to experimental error.

The above derivation was conducted for the system indicated in Figure 5, that does not have a solution resistance (the derivation would apply also to results obtained with an ideally solution resistance-compensated system imposing a constant potential scan rate at the interface). The case of a finite solution resistance (Figure 7) with the potential ramp applied to the entire circuit is much more complicated¹ and will not be addressed here. However, cases in which the solution resistance was not compensated but was of comparatively small value (as it was the case in the specimens examined here) may be analyzed with approximate treatment shown in Appendix 1.

Appendix 2 summarizes the procedure to evaluate CYCPR experiments based on the above treatment and approximate correction for small solution resistance effects.

Application to the experimental results

Eqs. (7) and (9) were applied to the cyclic polarization results, after adjustment for the small solution resistance effects per Appendix 1. The results are presented in Table 1, showing generally good agreement between the CPE parameter values obtained by EIS and those obtained with the time domain data. Repeat tests provided consistent results. Since the current measurements were performed at the end of the potential scans, spurious effects from the initial current jump sometimes observed upon initiation of potentiostatic control were minimized. The results provided good differentiation between the behavior of the plain steel and galvanized specimens. Discussion of the relative performance and characteristics of these materials has been presented elsewhere.^{1-3;8}

Application of Eq.(10) yielded values of R_p that are compared in Table 2 with those obtained by EIS, as well as with the values of R_{pa} obtained by examination of the slope of the V-I curves at the end of the downward excursion and correcting for solution resistance.

The R_p values estimated by CYCPR approximated reasonably well those obtained by EIS, considering the large margin of relative error (typically a factor of 2) inherent to the EIS data fitting procedure when the admittance corresponding to R_p is very small compared with that of the CPE. The R_{pa} values obtained at the lowest scan rate (0.0125 mV/s) were close but consistently lower than the R_p values obtained by CYCPR, while the R_{pa} values for 0.05 mV/s were typically several times smaller than the R_p obtained by CYCPR. This was as expected since the slope of the V-I curve at the point where R_{pa} was obtained should reflect not only the current demand from the polarization resistance, but also still significant current demand from the CPE. The better approach at the lowest scan rate was also as expected since the CPE currents should become less important as the scan rate decreases.

The specimens examined here were in the passive condition and probably corroding at extremely small rates. At the slow scan rates used in these experiments, even the smallest R_{pa} values in Table 2 would correspond to apparent corrosion rates normally associated with passive behavior.⁵ However, if faster tests were used, excessive underestimation by R_{pa} and possible misdiagnosis of the corrosion state could result. If the purpose of the tests were quantitative estimation of very small corrosion rates (for example in attempting to evaluate the durability of thin galvanized layers⁸), then the use of the R_{pa} values would be inappropriate even in the conditions of Table 2. The alternative CYCPR procedure may in those cases provide a more accurate estimate of the corrosion condition of the system, at least in those cases in which an R_p -CPE combination is mechanistically justified.

The procedure developed above and summarized in Appendix 2 is based on a simplified model of a slowly corroding interface, and subject to numerous limitations. The calculations assumed that a finite polarization resistance existed, and that the only other component in the interfacial impedance was provided by an ideal CPE. No consideration has been given to the possible presence of various factors including the following: diffusional limitation of one or more of the reactions involved in the corrosion process; non-negligible reverse reactions, excitation current inhomogeneities, corrosion macrocells and localized corrosion, non-linear response, and dielectric behavior of the concrete. Considerations of those and other factors is critical in interpreting the results of the calculations, and the reader is referred to previous publications in the field.¹⁴⁻¹⁷

If R_s is a large compared with the other interfacial impedance elements the simplified approach used in Appendix 1 is no longer appropriate. In that case, numerical solutions of the problem may be used in conjunction with a fitting procedure, more complicated than the procedure described here. Possible approaches to the more general case of large R_s have been described in other papers of this series.¹⁻³

No mechanistic assumptions have been made about the origin of the CPE behavior, which is in itself only approximately valid in a relatively restricted frequency interval. Preliminary examination of the EIS behavior suggested that a more accurate representation of the processes not directly associated with net metal dissolution may include the combination of a diffusional impedance in series with a large ideal capacitance. In that case, the system may already have a finite (although very large) polarization resistance at the low frequency limit, even when CPE-only behavior is closely approached at intermediate frequencies (mHz range) and the present analysis would suggest infinitely large R_p . Work is in progress to examine this possibility with available models on the EIS response of passive films¹⁷, and to improve the interpretation procedure accordingly.

CONCLUSIONS

1. A simple procedure was introduced for evaluating the parameters of a slowly corroding interface that may be represented by the parallel combination of a polarization resistance and a CPE.
2. In fully solution resistance-compensated experiments the procedure uses only four measured currents in two separate one-cycle polarization resistance tests performed at different potential scan rates.
3. In experiments with no solution resistance compensation but low solution resistance values, the procedure requires only one independent measurement of the solution resistance with a three-point A.C. resistance meter.
4. The procedure was demonstrated with measurements performed with passive plain and galvanized steel specimens in concrete.

ACKNOWLEDGMENTS

The authors are indebted to the Florida Department of Transportation for partial support of this investigation. The opinions and findings in this paper are those of the authors and not necessarily those of the funding agencies. One of the authors (E.I.M.) acknowledges the scholarship provided by the National Council of Science and Technology (CONACYT-México).

Appendix 1 - Approximate compensation for the presence of a small ohmic potential drop.

Eqs.(7) and (9) do not apply strictly to the data in Figures 3 and 4 since those tests were not conducted using ohmic resistance compensation. Consequently, \dot{V} at the steel concrete interface varied from the constant value \dot{V}' imposed externally at the reference electrode position. V_{MAX} was likewise different from V'_{MAX} , the externally applied maximum potential deviation. However, for much of the test the ohmic potential drop was small compared to the potential at the interface, which permitted proposing the following approximation to equivalent values of V_{MAX} and \dot{V} given that R_s was known independently (from routine measurements with a fixed-frequency AC resistivity meter, and confirmed by the EIS experiments). The actual value of V_{MAX} can thus be estimated as

$$V_{MAX} \approx V'_{MAX} - I_D R_s \quad (A1)$$

The return to the initial interface potential does not take place at $T' = -2 V'_{MAX} / \dot{V}'$ because of the potential drop resulting from R_s and the terminal current I'_E obtained at $t=T'$. Instead, the potential cycle at the interface is completed at an estimated $T \approx T' + I'_E R_s / \dot{V}'$. Therefore, on first approximation the average scan rate was estimated as

$$\dot{V} \approx \dot{V}' (1 - I_D R_s / V'_{MAX}) / (1 - 0.5 I'_E R_s / V'_{MAX}) \quad (A2)$$

Finally, the terminal current I_E for completion of the actual cycle was estimated by graphically extending the return scan to a potential that exceeded the starting potential by $I'_E R_s$ and reading the corresponding value in the current axis.

Appendix 2 - Summary of the procedure to obtain the system parameters from the CYCPR results.

Procedure when using measurements with ohmic potential drop compensation that provide a true constant potential scan rate.

1. Two cyclic polarization experiments A and B at different potential scan rates are required (see Figure 8, illustrating the case of a cathodic excursion experiment)
2. From each experiment, it is necessary to record the chosen potential scan rate \dot{V} , the chosen maximum potential deviation V_{MAX} , and the measured currents I_D and I_E . Thus, this procedure requires only knowing four experimentally measured currents since the other variables are imposed..
3. Evaluate n and Y_o using Eqs. (7) and (9) respectively.
4. Evaluate R_p using Eq.(10) for experiments A and B.

Procedure when using measurements without ohmic potential drop compensation but where the solution resistance effect is small.

1. Two cyclic polarization measurements are required as in the previous procedure. In addition, a measurement of the solution resistance R_s is required (as indicated in the Experimental section).
2. From each experiment it is necessary to record R_s , the potential scan rate \dot{V}' and the maximum excursion V'_{MAX} imposed by the equipment at the reference electrode position, and the currents I_D and I'_E measured when $V' = V'_{MAX}$ and $V' = 0$ (at the end of the test), respectively. Thus, 5 measured magnitudes (one obtained by graphic extrapolation) are required for this procedure.
3. Calculate V_{MAX} and \dot{V} using Eqs.(A1) and (A2) respectively.
4. Calculate I_E by extrapolating the V' I curve as shown in Figure 9.
5. Evaluate n and Y_o using Eqs. (7) and (9) respectively.
6. Evaluate R_p using Eq.(10) for experiments A and B.

Table 1
Average CPE Parameters and Solution Resistance Obtained by EIS and CYCPR

SPECIMEN, TYPE (GX,PX) [†]	E _{CORR} (mV-CSE) [‡]	Y _o (Ω ⁻¹ s ⁿ) (EIS)	Y _o (Ω ⁻¹ s ⁿ) (CYCPR)	n (EIS)	n (CYCPR)	Rs* (Ω) (EIS)	Rs* (Ω) (CYCPR)
BBW1 (P1)	-73	1.20 10 ⁻²	1.14 10 ⁻²	0.84	0.85	810	680
BCW1 (P2)	-60	1.07 10 ⁻²	1.67 10 ⁻²	0.86	0.94	1730	1500
GBW1 (G1)	-341	2.44 10 ⁻³	2.32 10 ⁻³	0.69	0.72	1050	840
GCW1 (G2)	-369	2.16 10 ⁻³	1.41 10 ⁻³	0.72	0.65	1690	1380
GDW1 (G3)	-475	3.03 10 ⁻³	3.48 10 ⁻³	0.65	0.70	2810	2270

(Specimen area ≈ 80 cm²)

*Rs values for EIS were obtained for best fit to the CPE Randles' mode, using frequencies < 0.1 Hz. Rs values for the CYCPR tests were measured independently as shown in the Procedure.

[†]G:Galvanized; P:Plain steel, X= 1, 2, 3 designates the corresponding concrete mix.

[‡]Cu-CuSO₄ electrode.

Table 2
Averaged* Rp and Rpa Values

SPECIMEN, TYPE (GX,PX) [†]	CYCPR SCAN RATE (mV/s)	Rp (EIS) (Ω)	Rp (CYCPR) (Ω)	Rpa (Ω)
BBW1 (P1)	.0125	2.6 10 ⁵	1.7 10 ⁵	0.68 10 ⁵
	.050		1.2 10 ⁵	0.28 10 ⁵
BCW1 (P2)	.0125	3.1 10 ⁵	2.1 10 ⁵	1.1 10 ⁵
	.050		5.7 10 ⁵	0.39 10 ⁵
GBW1 (G1)	.0125	1.9 10 ⁵	0.93 10 ⁵	0.54 10 ⁵
	.050		0.96 10 ⁵	0.30 10 ⁵
GCW1 (G2)	.0125	1.6 10 ⁵	2.4 10 ⁵	0.69 10 ⁵
	.050		3.0 10 ⁵	0.40 10 ⁵
GDW1 (G3)	.0125	0.54 10 ⁵	0.35 10 ⁵	0.26 10 ⁵
	.050		0.24 10 ⁵	0.14 10 ⁵

(Specimen area ≈ 80 cm²)

*Inverse of average Rp⁻¹ and Rpa⁻¹.

[†]G:Galvanized; P:Plain steel, X= 1, 2, 3 designates the corresponding concrete mix.

REFERENCES

1. A. Sagüés, S. Kranc, E. Moreno, *Corros. Sci.*, 37, 7 (1995): p. 1097.
2. A. Sagüés, S. Kranc, E. Moreno, *Electrochim. Acta*, 41, 7/8 (1996):p. 1239.
3. A. Sagüés, S. Kranc, E. Moreno, *Electrochim. Acta*, 41, 16 (1996):p. 2661.
4. F. Mansfeld, in *Advances in Corrosion Science and Technology*, Vol. 6, eds. M. Fontana and R. Staehle (New York, NY: Plenum Press, 1976), p.
5. C. Andrade, M.C. Alonso, in *Application of Accelerated Corrosion Tests to Service Life Prediction of Materials*, ASTM STP 1194, eds. G. Cragolino, N. Sridhar (Philadelphia, PA: ASTM, 1994), p. 282.
6. D. Macdonald, *J. Electrochem. Soc.*, 125 (1978): p. 1051.
7. H. Shih, H. Pickering, *J. Electrochem. Soc.*, 134 (1987): p. 1943.
8. E. Moreno, A. Sagüés, R. Powers, "Performance of Plain and Galvanized Reinforcing Steel during the Initiation Stage of Corrosion in Concrete with Pozzolanic Additions," *CORROSION/96*, paper no. 326 (Houston, TX: NACE, 1996).
9. P. Castro, A. Sagüés, E. Moreno, L. Maldonado, L. Genescá, *Corrosion*, 52, 8 (1996): p. 609.
10. C. Naish, A. Harker, R. Carney, in *Corrosion of Reinforcement in Concrete*, eds. C. Page, K. Treadway, and P. Bamforth (London, UK: Elsevier Applied Science, 1990), p. 314.
11. A. Sadkowski, *Electrochim. Acta*, 38 (1993): p. 2051.
12. F. H. van Heuveln, *J. Electrochem. Soc.*, 141 (1994): p. 3423.
13. S. Goldman, in *Transformation Calculus and Electrical Transients* (Englewood Cliffs, NJ: Prentice-Hall, 1955).
14. A. Sagüés, "Electrochemical Impedance of Corrosion Macrocells on Reinforcing Steel in Concrete," *CORROSION/90*, paper no. 132 (Houston, TX: NACE, 1990).
15. K. Lawson, N. Thompson, M. Islam, "Influence of Macro-cell Corrosion on Corrosion Measurements of Concrete Structures," *CORROSION/94*, paper no. 310 (Houston, TX: NACE, 1994).
16. A. Sagüés, "Corrosion Measurement Techniques for Steel in Concrete," *CORROSION/93*, paper no. 353 (Houston, TX: NACE International, 1993).
17. D. Macdonald, *Electrochim. Acta*, 35 (1990): p. 1509.

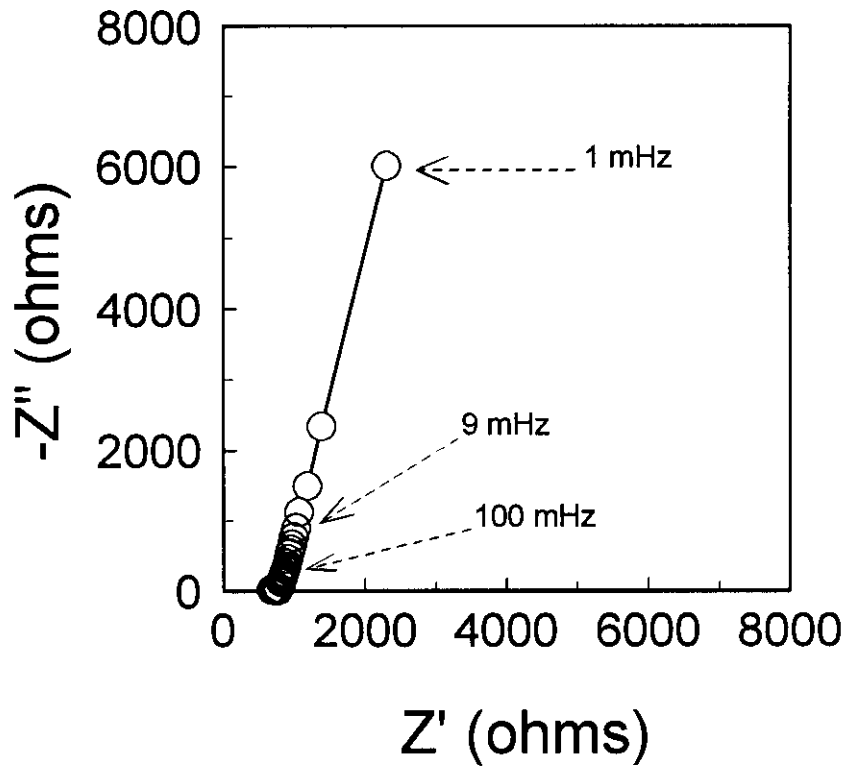


FIGURE 1. EIS Results for Specimen BBW1 (Plain Steel Rebar).

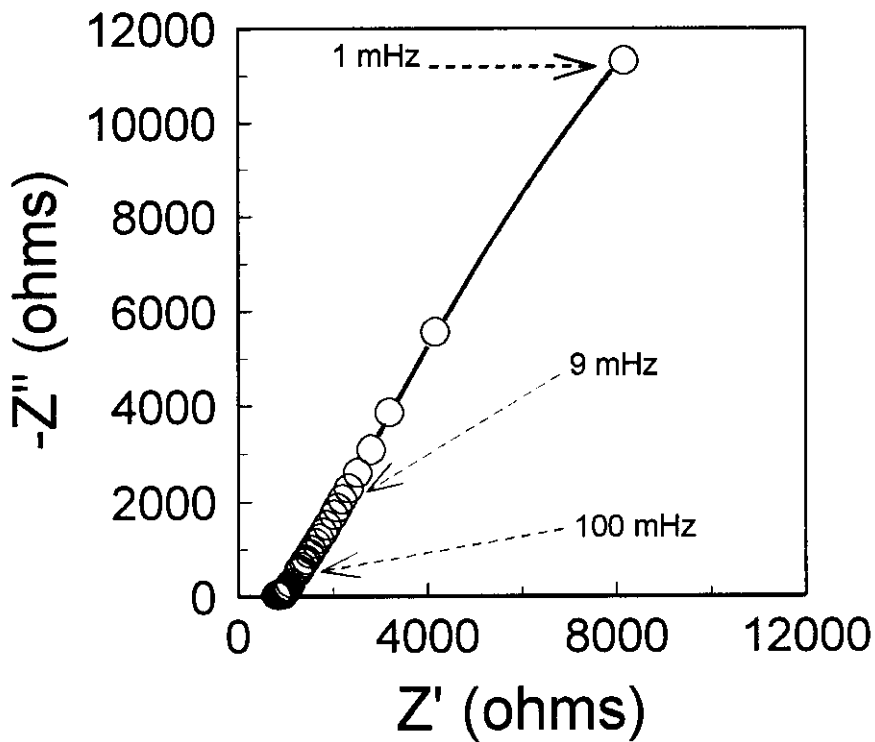


FIGURE 2. EIS Results for Specimen GBW1 (Galvanized Rebar).

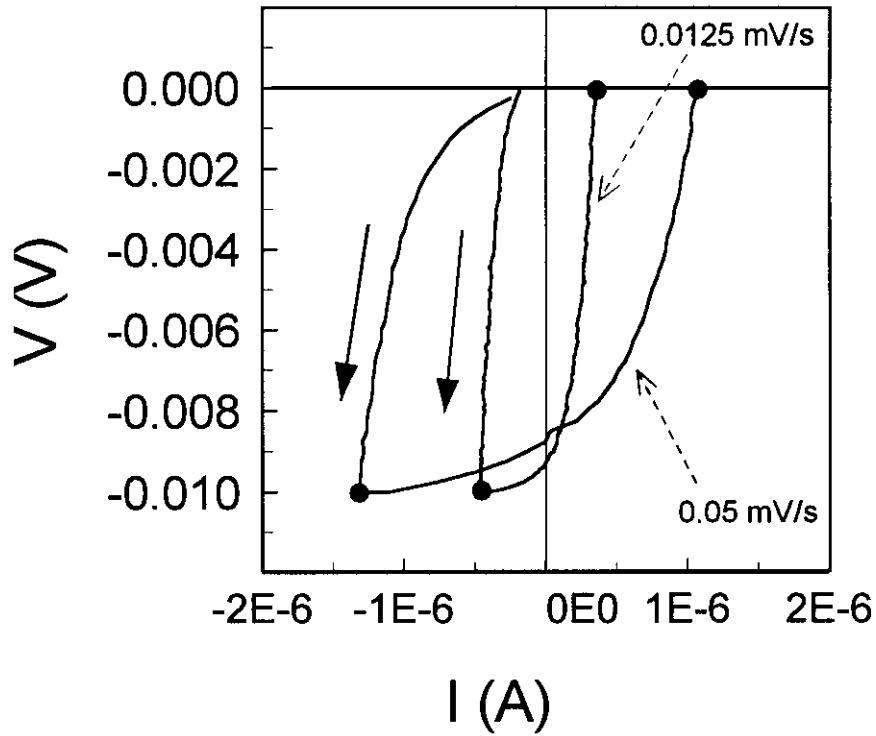


FIGURE 3. CYP Results for Specimen BBW1 (Plain Steel Rebar).

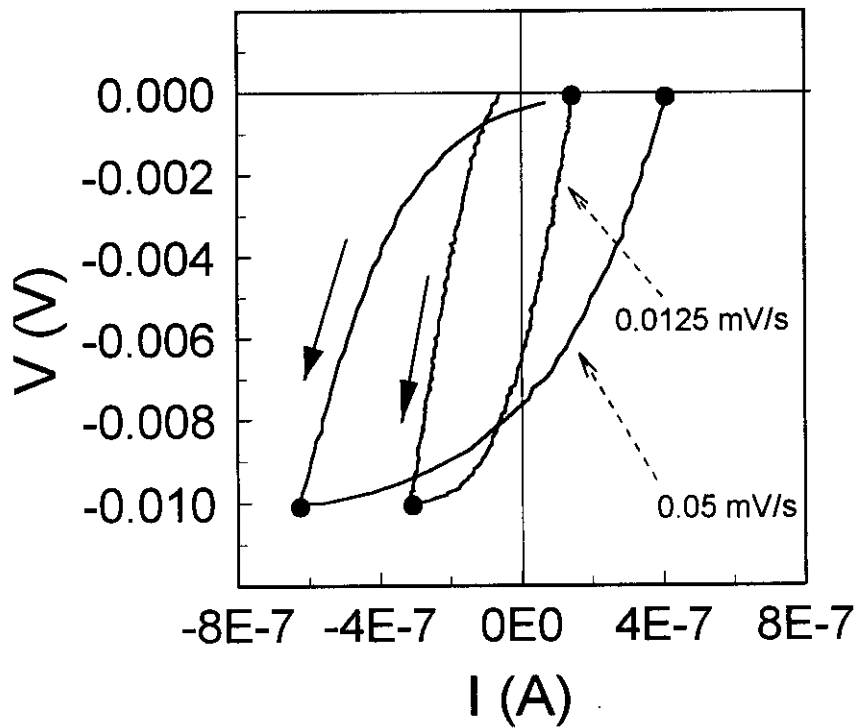


FIGURE 4. CYP Results for Specimen GBW1 (Galvanized Rebar).

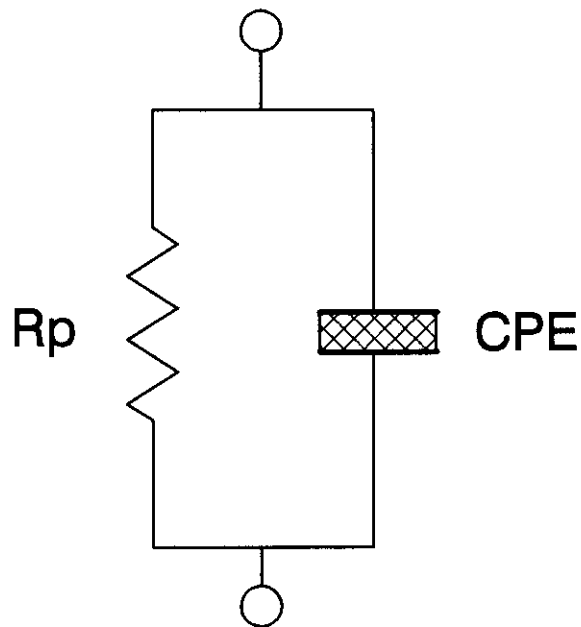


FIGURE 5. Equivalent Circuit Representation of a Metal-Electrolyte Interface Meeting the Assumptions of the Theoretical Derivation.

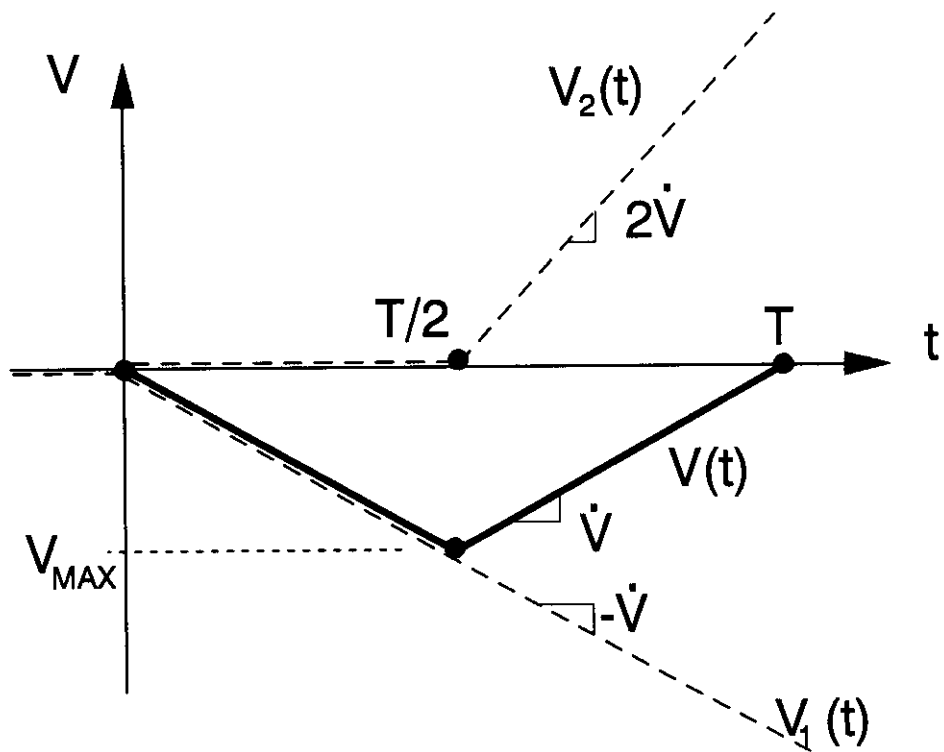


FIGURE 6. Potential Excitation Schedule During a CYCPR Test.

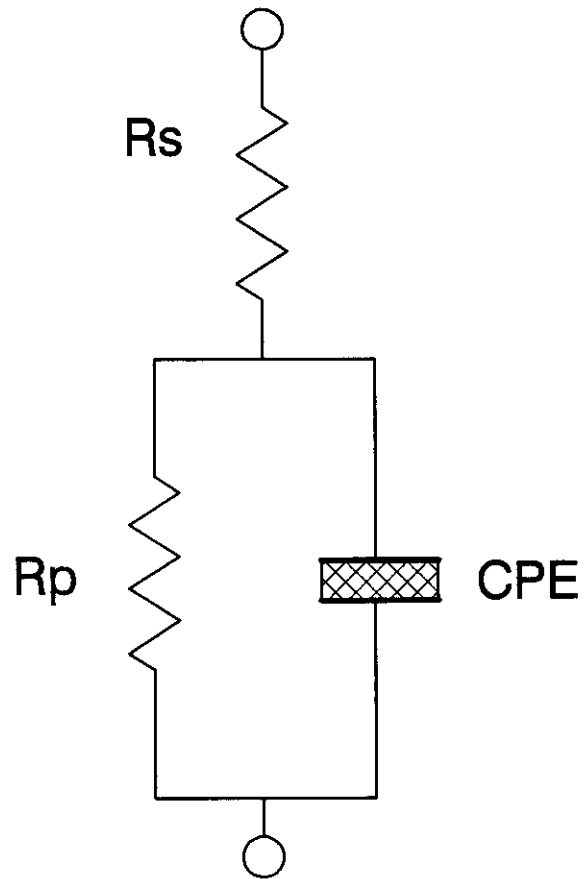


FIGURE 7. System With Finite Solution Resistance.

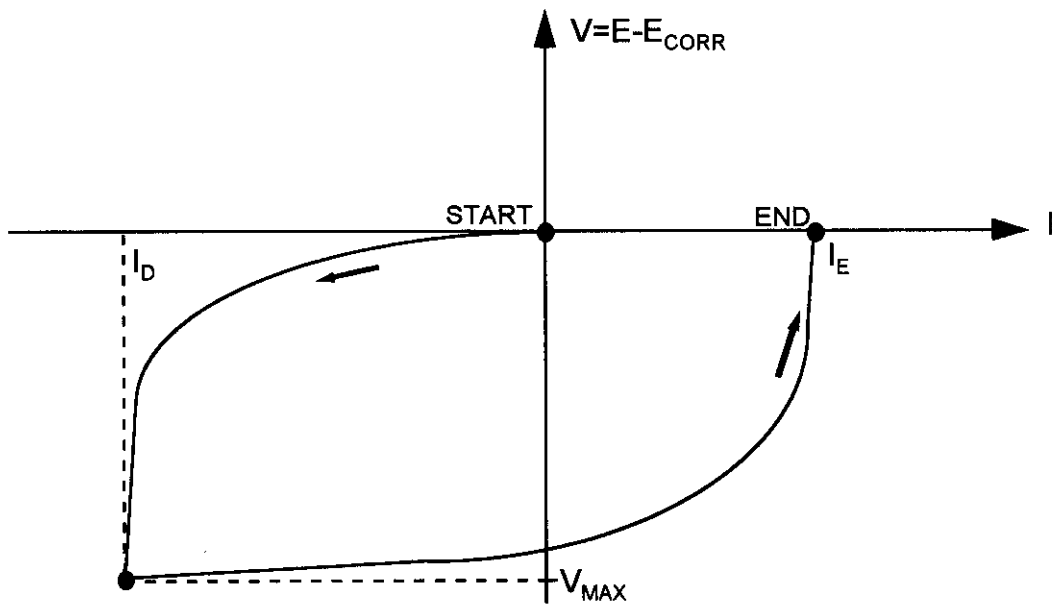


FIGURE 8. Schematic of Magnitudes Used in Evaluating Results of a CYCPR Test. (See Appendix 2).

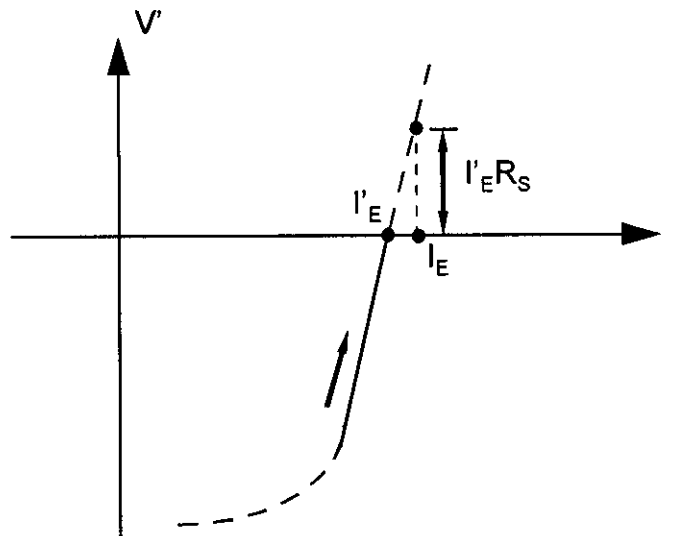


FIGURE 9. Estimation of I_T for the Case of Small R_s Values.